Available online at www.sciencedirect.com

ScienceDirect

Physics Procedia 14 (2011) 67–72

Physics Procedia

9th International Conference on Nano-Molecular Electronics

Probing of Transient Electric Field Distribution in ITO/PI/P3HT/Au By Time-Resolved Optical Second Harmonic Generation Measurement

Ryo Miyazawa, Dai Taguchi, Takaaki Manaka, and Mitsumasa Iwamoto1*

Department of Physical Electronics, Tokyo Institute of Technology, 2-12-1 O-okayama, Meguro-ku, Tokyo, 152-8552, Japan

Abstract

By using time-resolved optical second harmonic generation (TR-SHG) measurements, we studied carrier behaviors in poly(3-hexylthiophene) (P3HT) metal-insulator-semiconductor (MIS) diodes. TR-SHG measurements probed transients of electric field distribution in the P3HT active layer. Results showed that hole injection and removal processes were non-reversal, where the response times were different from each other and the relaxation time of the transient electric field strongly depended on the hole injection process.

Keywords: Transient, P3HT, MIS diodes, SHG;

1. Introdution

The discovery of highly conducting organic materials [1], e.g., pentacene, polythiophene, etc. has resulted in studies of their possible applications to organic electronics devices, such as organic electroluminescent devices (OLEDs), organic solar cells and organic field-effect transistors (OFETs) [2]. The study of the nature of organic materials with a low carrier density has already shown the importance of the injected carrier behavior [3],[4]. Recent studies have revealed that carrier injection process dominates the operation of OFETs [5]. By using optical SHG measurements, we directly probed space charge field formation process caused by injected carriers [6]. Analyzing pentacene OFETs as a system of Maxwell-Wagner effect elements, we discussed the OFET characteristics in terms of injected carrier behaviors [7],[8]. We have also employed electric-field-induced SHG (EFISHG) in MIS diodes with an organic semiconductor layer of P3HT to study the electric field distribution in steady states. Results showed

* Corresponding author. Tel.: +3-5734-2562; fax:+3-5734-2191.
E-mail address: iwamoto@pe.titech.ac.jp.

1875-3892 © 2011 Published by Elsevier Ltd. Open access under CC BY-NC-ND license.
doi:10.1016/j.phpro.2011.05.015

that electrons generated in the P3HT layer by photoillumination were trapped as excess charges in the MIS structure at the P3HT-inulstor interface [9]. The capacitance-voltage (*C-V*) measurements supported the results. However, the detailed discussion about transient charge movement has not yet been done yet. In this study, using TR-SHG measurements, we studied the transient electric field distribution in a P3HT active layer of the MIS diodes. The measurements were carried out at two conditions, i.e., in the region where a P3HT layer functioned as an insulator and in the region where a P3HT layer acted as a conductor.

2. Experimental

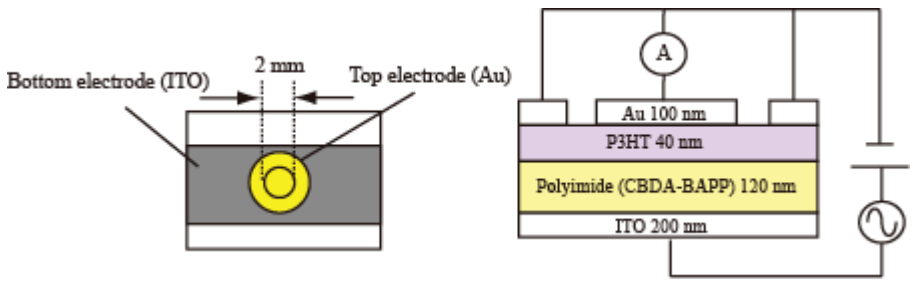

Fig. 1 Schematic diagram of an MIS structure.

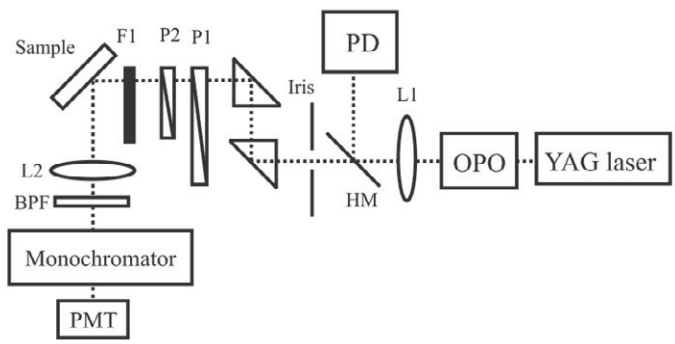

Fig. 2 Schematic diagram of experimental setup for TRM-SHG.

We used P3HT as the active layer (semiconductor) of MIS diodes, where Au and indium tin oxide (ITO) were electrodes (see Fig. 1). The polyimide insulator (120 ± 20 nm thickness) was prepared by using thermally imidized polyamic acid derived from cyclobutane dianhydride and 2,2-bis(4-aminophenoxyphenyl) propane (CBDA-BAPP PI), and it was deposited by spin-coating (2100 rpm, 1.5 min). After the deposition, the layer of the PI's precursor was annealed at 90 ° C for 30 min and then at 260 ° C for 2 hours. Subsequently, the P3HT layer was deposited by spin-coating method (2100 rpm, 20 s) from a 0.5 wt% P3HT solution with chloroform. After deposition of the P3HT layer, the sample was annealed at 120 ° C. The top Au electrode was evaporated at a pressure of less than 6×10^{-6} Torr. The thickness of the Au electrode was 100 nm. The working centered-electrode area was 3.1 mm^2. The electrode was surrounded by a guard ring to eliminate lateral current. Figure 2 portrays the experimental setup used for the TR-SHG measurement. The light source was a Nd:YAG laser coupled with an optical parametric oscillator. The incident light (1060 nm) impinged on the sample from the ITO side at an angle of 45 °, and the reflected light through monochromator was detected using a photomultiplier tube. The wavelength of detected light was 530 nm where the voltage dependence of the SHG signal generated from P3HT was intensively observed [10]. The intensity of SHG signal I_{SHG} is proportional to $|\chi^{(3)}E_{(0)}\,E_{(\omega)}E_{(\omega)}\,|^2$. Here, $E_{(0)}$ is the internal electric field in P3HT and $E_{(\omega)}$ is the electric field intensity of incident light. $\chi^{(3)}$ is the third order susceptibility tensor dependent on the light wavelength and is determined by intrinsic material property. Therefore, the I_{SHG} from P3HT layer can be detected selectively

even if P3HT is inside the multiple layer system. Impedance measurements were also conducted using an LCR meter in dark. The applied AC amplitude and frequency were 0.1 V and 1 kHz, respectively. All measurements were conducted in N_2 atmosphere in dark .

3. Results and Discussion

3.1 *C-V* and *C-F* measurements

Figure 3 shows the typical *C-V* and *C-F* characteristics of the MIS diode. We classified the *C-V* characteristics into three regions, a conductor region (V_{DC} < -5 V), an insulator region (0 V < V_{DC}) and an intermediate region between conductor and insulator region (-5 V < V_{DC} < 0 V). The capacitances in the conductor region and in the insulator region correspond to the capacitance of PI single layer and the series capacitance of PI and P3HT layer, respectively [11]. Results showed that the injected carriers (holes) accumulated at the P3HT/PI interface in the conductor region, and the P3HT was an ideal insulator being free from holes in the insulator region. In the intermediate region, the thickness of the insulator region in the P3HT layer changed accordingly with the applied voltage. According to the *C-F* characteristics, the capacitance in the conductor region decreased from 1 kHz, indicating that holes did not follow the alternating voltage, while the capacitance in the insulator region showed no dependence on frequency in this frequency region.

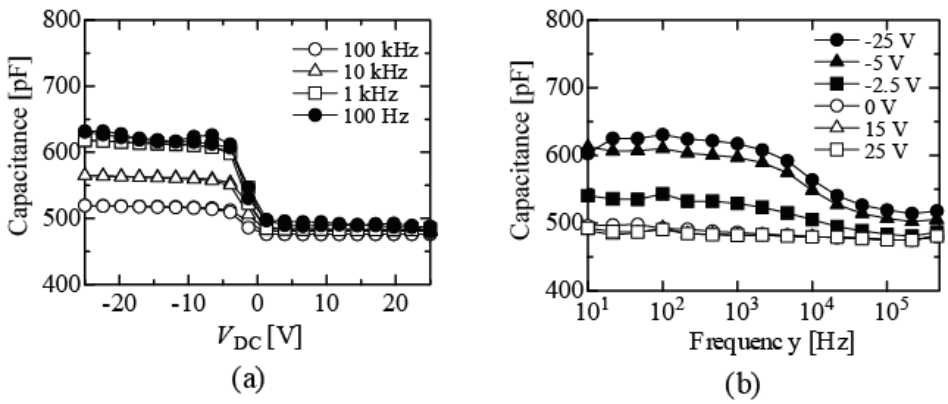

Fig. 3 (a) Typical *C-V* characteristics of the MIS diode in applying V_{AC} of various frequency, (b) Typical *C-F* characteristics of the MIS diode in applying various V_{DC} measurement

3.2 TR-SHG measurements

According to the result of C-V measurements, we carried out TR-SHG measurements for two cases; insulator region and conductor region.

3.2.1 Insulator region

Figure 4(a) portrays the transient SHG signal generated from the P3HT layer before and after applying voltage (0 V < V_{DC}). The transient SHG signal traces changes of the electric field in the P3HT. After application of voltage, the SHG intensity increased rapidly with a response time of 45 ns, corresponding to the circuit time constant R_sC^*. Here, R_s is the resistance of Au, ITO electrodes and the lead wire of the circuit. C^* is the series capacitance of PI and P3HT layer. After that, the SHG intensity saturated. On the other hand, when we removed the applied voltage (V_{DC} = 0 V), the SHG decayed reversely with a response time of 59 ns. The results suggested that there was no carrier injection into the P3HT layer, where the P3HT layer was working as an insulator, and charging and discharging onto electrodes were observed. To further confirm these charging and discharging processes, we measured the TR-SHG by connecting external resistance R, 1 kΩ and 10 kΩ, to the Au electrode. Figure 4(b) shows the results, where the response time changes in accordance with the connected external resistance. Table 1 and 2 are the relaxation times

and the lead resistance respectively. Here, we chose the capacitance at V_{DC} = 25 V and f = 1 MHz as the capacitance C^* (=5.0 $\times 10^2$ pF). The table showed the contact resistance was around 1.1 $\times$ 10^2 Ω.

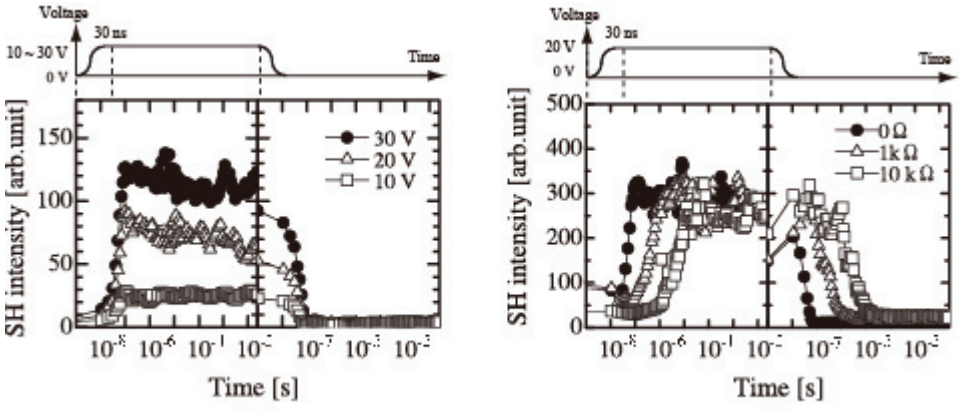

Fig. 4 (a) Variation of SHG signal from an P3HT layer after applying voltage, (b)Variation of SHG signal from an P3HT according to the external resistance.

Tab. 1 Relaxation time τ

	0 Ω	1 kΩ	10 kΩ
Charging process	4.5×10^{-8} s	2.3×10^{-7} s	2.1×10^{-6} s
Discharging process	5.9×10^{-8} s	5.8×10^{-7} s	8.9×10^{-6} s

Tab. 2 Evaluation for contact resistance connected in series to sample

	0 Ω	1 kΩ	10 kΩ
Charging process	9.6×10^{1} Ω	5.1×10^{2} Ω	4.7×10^{3} Ω
Discharging process	1.3×10^{2} Ω	1.3×10^{3} Ω	2.0×10^{4} Ω

3.2.2 Conductor region

Figure 5 shows the transients of SHG signals and variation of electric fields in the P3HT layer before and after applying pulse-voltages. The *C-V* characteristics suggested the presence of no electric field in the P3HT layer in the conductor region, but the static SHG signals were generated, possibly due to the noise signals from the ITO and Au layers. After subtracting these effects from the original EFISHG signals, the square root of the signals were plotted in Fig. 5(b) to represent the electric field change Δ E_{P3HT}.Note that the sample used here was different from that used for Fig. 3, but the *C-V* and *C-F* characteristics were nearly the same as those in Fig. 3. In the hole removal process of Fig. 5(b), after applying a DC voltage V_{DC}, the electric field changed dramatically with one peak and saturated within 10^{-6} s. These results indicated that the charges accumulated on both electrodes and formed electric field in the P3HT layer. Subsequently, charges in the PI/P3HT interface were transferred to the Au electrode by the formed electric field. Accordingly, the electric field in the P3HT layer decreased. The peak height showed no bias dependence, possibly because the hole removal process was enhanced by applying higher voltage. In other words, the removal speed increased as applied voltage increased, which resulted in the generation of peaks with no relation

of applied voltage. On the other hand, in the hole injection process of Fig. 5(a), the SHG intensity of -20 and -25 V started to increase at around 10^{-7} s because the SHG from the P3HT layer canceled out SHG from Au and ITO, whose phase coincided with SHG from the P3HT layer. For the same reason, SHG intensity of -20 and -25 V started to increase at around 10^{-6} s. In Fig. 5(b), the electric field changed significantly with one peak and saturated within around 10^{-5} s. The peaks suggested that holes and electrons accumulated on both electrodes after application of voltage and they formed electric field in the P3HT layer. Subsequently, the holes injected into the P3HT layer and accumulated at the PI/P3HT interface. As a result, the electric field in the P3HT layer decreased to zero. The peak value of electric field increased by increasing applied voltage, but that was not proportional to the voltage because holes were injected into the P3HT layer before fully charging at both electrodes. The response time of the hole injection process was about 10 times longer than that of the hole removal process. This fact indicated that carrier motions were mainly ruled by injection process.

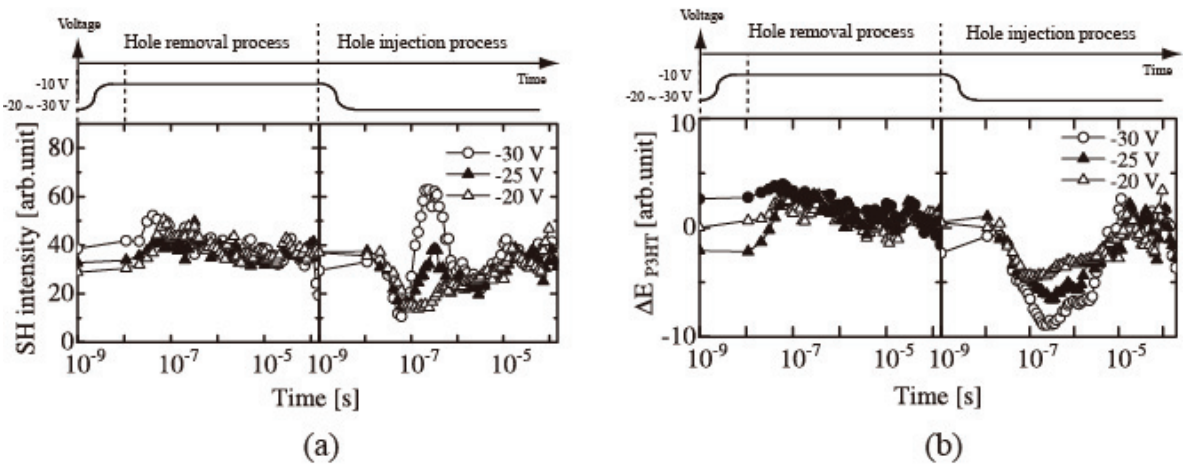

Fig. 5(a) SHG signal and (b) variation of electric field in P3HT layer after application of voltage.

4. Results and Discussion

We observed transients of SHG signals in two conditions of P3HT, the insulator condition and conductor condition to study the carrier motions in MIS diodes with an P3HT layer. In the insulator region, the induced charges by the application voltage formed an electric field in the P3HT, and the relaxation time corresponded to the time constant of circuit (R_sC^*). On the other hand, in the conductor region, the relaxation time difference in hole injection process and in hole removal process was observed. This difference indicated that injection process strongly affected the relaxation times.

[1] C. D. Dimitrakopoulos and P. R. L. Malenfant: Adv. Mater. **14** (2002) 99.
[2] S. R. Forrest: Nature **428** (2004) 911.
[3] W. Brütting, S. Berleb, and A. G. Mückl: Org. Electron. **2** (2001) 1.
[4] M. A. Lampert, and P. Mark: Current Injection in Solids (Academic, New York, 1970).
[5] Conjugated Polymer and Molecular Interfaces: Science and Technology for Photonic and Optoelectronic Applications, ed. W. R. Salaneck, K. Seki, A. Kahn, and J. -J. Pireaux (Marcel Decker, Inc, New York, 2001).
[6] T. Manaka, E. Lim, R. Tamura, and M. Iwamoto: Nat. Photonics **1** (2007) 581.
[7] R. Tamura, E. Lim, T. Manaka, and M. Iwamoto: J. Appl. Phys. **100** (2006) 114515.
[8] D. Yamada, T. Manaka, E. Lim, R. Tamura, M. Weis, and M. Iwamoto: J. Appl. Phys. **104** (2008) 074502.

[9] R. Miyazawa, D. Taguchi, T. Manaka, M. Iwamoto: IEICE Trans. Electron. **94** (2011) 185.
[10] Y. Shibata, M. Nakao, T. Manaka, E. Lim, and M. Iwamoto: Jpn. J. Appl. Phys. **48** (2009) 021504.
[11] R. Miyazawa, D. Taguchi, M. Weis, T. Manaka, and M. Iwamoto : Jpn. J. Appl. Phys. **49** (2010) 04DK07.